Crystallinity Morphology and Dynamic Mechanical Characteristics of PBT Polymer and Glass Fiber-Reinforced Composites

Chan-Seok Park,[1] Ki-Jun Lee,[1] Seong Woo Kim,[2] Young Kwan Lee,[3] Jae-Do Nam[3]

[1]*Department of Chemical Engineering, Seoul National University, Seoul, South Korea*
[2]*Department of Chemical Engineering, Kyonggi University, Suwon, Korea*
[3]*Division of Chemical Engineering, Department of Polymer Science & Engineering, Polymer Technology Institute, Sung Kyun Kwan University, Suwon, Korea*

Received 31 December 2001; accepted 30 January 2002

ABSTRACT: The crystalline morphologies of PBT (poly butylene terephthalate) and its glass fiber reinforced composite systems were investigated in a thin-film form by polarized optical microscopy and wide-angle X-ray diffraction. Three different types of PBT morphology were identified in the Maltese cross pattern: 45° cross pattern (usual type) by solvent crystallization, 90° cross pattern (unusual type) by melt crystallization at low crystallization temperature, and mixed type by melt crystallization at crystallization temperatures higher than 160°C. The glass fibers increased the number density of spherulites and decreased the size of crystallites acting as crystallization nucleation sites without exhibiting trans-crystallinity at the vicinity of the glass fiber surfaces. Finally, the storage modulus was analyzed by using a dual-phase continuity model describing the modulus by the power-law sum of the amorphous- and crystalline-phase moduli. The crystalline-phase modulus was extracted out from the PBT polymer and composite systems containing different amount of crystallinity. © 2002 Wiley Periodicals, Inc. J Appl Polym Sci 86: 478–488, 2002

Key words: morphology; X-ray; mechanical properties; PBT; viscoelasticity

INTRODUCTION

The bulk properties of crystalline thermoplastic composite materials are usually affected not only by individual properties of the polymer matrix and fiber reinforcements but also the processing conditions of time and temperature, which often affect the crystalline morphology of the final parts.[1,2] Specifically, it has been known that PBT has two crystal phases α and β depending on processing conditions.[3–5] The molecular chain in the alpha form has the *gauche-trans-gauche* conformation in the glycol residues, whereas the beta form has the *trans-trans-trans* conformation under the strain and stress. In addition, as with other thermoplastic polymers such as poly(ether ether keton) and poly(ethylene vinyl acetate) copolymer, additional crystiallization can be obtained in PBT by physically aging the specimens.[6] Accordingly, the macroscopic mechanical deformation and thermal treatment history of PBT are closely associated with the morphology and residual-stress development in the final products of PBT polymer and its fiber reinforced composites.[7,8]

Correspondence to: J.-D. Nam (jdnam@skku.ac.kr).
Contract grant sponsor: Korea Science and Engineering Foundation; contract grant number: 96-0502-0601-3.

Journal of Applied Polymer Science, Vol. 86, 478–488 (2002)

The reinforcing fibers included in crystalline polymers often act as nucleating sites for crystallization.[1,9–14] When nucleation occurs at the fiber surface with a sufficiently high density, the crystallites may be obstructed to grow laterally and thus be constrained to columnar growth, where the columnar morphology is often referred to transcrystallinity. The existence of a transcrystalline zone has been reported to depend on the types of fibers, surface treatment, and polymers. Some organic fibers such as natural cellulose, cotton, carbon, and copper fibers, show transcrystalline growth.[1] The fiber surface treatment or sizing may also affect the development of transcrystallization.[15] In the case of glass fiber-reinforced thermoplastic composites, however, it is still argumentative in the existance of transcrystallinty around the surface of the glass fiber. It has been reported that the transcrystalline zone is not observed by microscopic investigations,[16–18] although the glass fiber increased the nucleation density. It has been recently shown that the transcrystalline zone appeared when the glass fiber is pulled out from polymer melt or when the shear stress is applied at the crystallization temperature.[19–22,23] In addition, the literature reports that glass fibers generated the transcrystallinity in PET and nylon matrix systems when their surfaces are specially treated with compatible polymers.[24]

In addition, the bulk structure or macrostructure of polymer depends on whether crystallization occurs

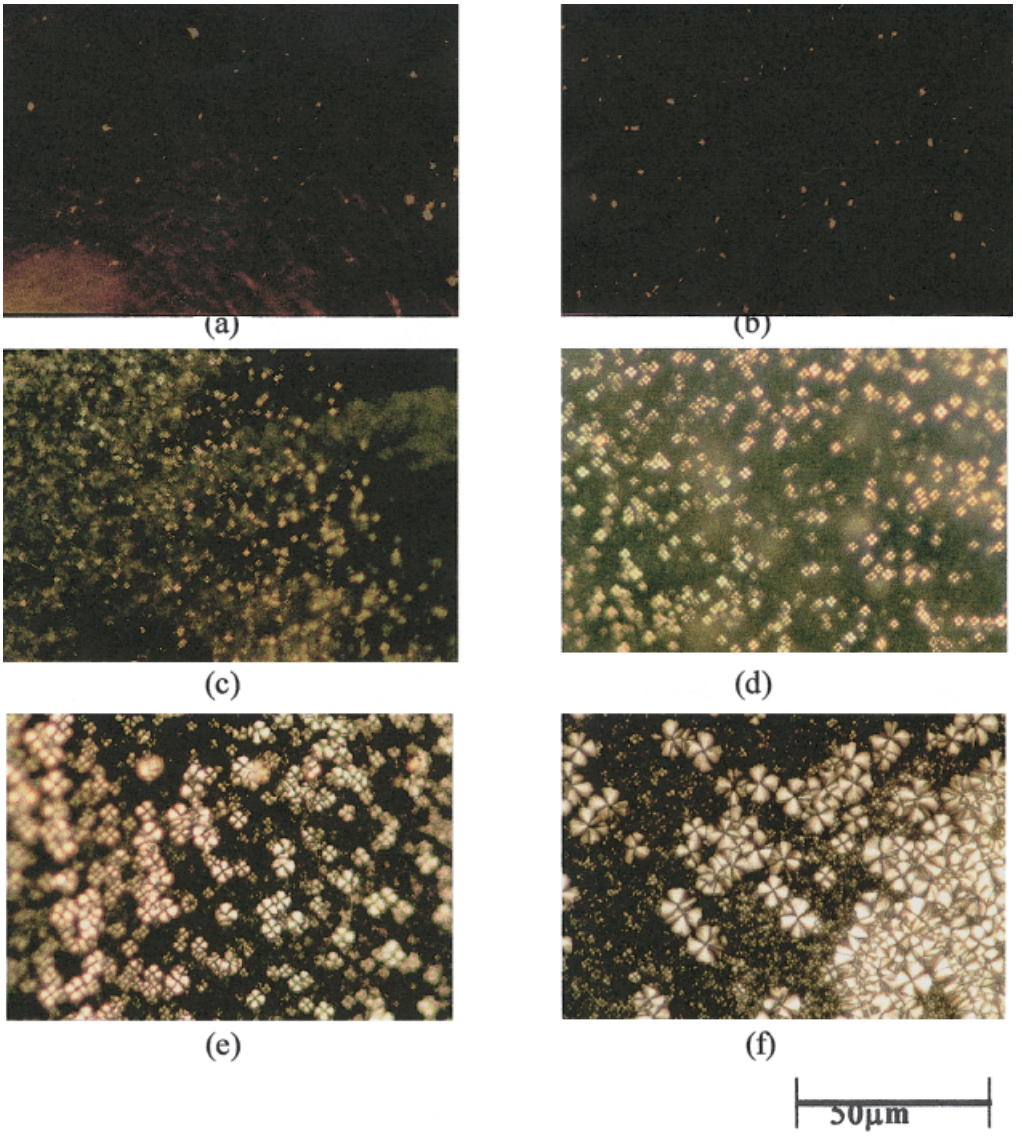

Figure 1 Polarized optical micrograph of PBT spherulites crystallized at the various isothermal temperatures: (a) 0°C, (b) 20°C, (c) 40°C, (d) 60°C, (e) 80°C, (f) 100°C, (g) 120°C, (h) 140°C, (i) 160°C, (j) 180°C, (k) 200°C, and from (1) solution. [Color figure can be viewed in the online issue, which is available at www.interscience.wiley.com.]

from dilute solution or melt. When crystallization occurs under quiescent conditions in a dilute solution, then single crystals arise with folded chains. When crystallization occurs from the melt under quiescent conditions, chain folding occurs rapidly in all directions, leading to a spherical structure, which is composed of a radiation array of fine fibrils, or the stacks of ribbon-like crystals.[25] The physical, mechanical, optical, and electrical properties of polymeric materials are usually affected by the quantity and orientation of crystalline phase. For example, such properties as density, heat of fusion, spectroscopic, and X-ray diffraction intensities depend on the level and anisotropy of crystallinity, which is usually affected by crystallization processing conditions. In addition, the mechanical strength, modulus, elongation and impact strength, and optical properties including birefringence and transmittance, vary with the crystalline morphology.[25,26]

In this study, the crystalline morphologies in PBT and its composites were investigated through polarized optical microscopy (POM), and the degree of crystallinity were measured by the wide-angle X-ray diffraction (WAXD) experiments as a function of crystallization temperature. The PBT and the glass fiber-reinforced PBT composites exhibited different types of spherulite morphology for different crystallization conditions, and subsequently their viscoelastic properties were correlated with the degree of crystallinity and the dual-phase continuity model.

EXPERIMENTS

The PBT samples (SKYTON) used in this study was provided by SK Chemical Co., Korea. Before the film preparation, the PBT pellets were dried in a vacuum

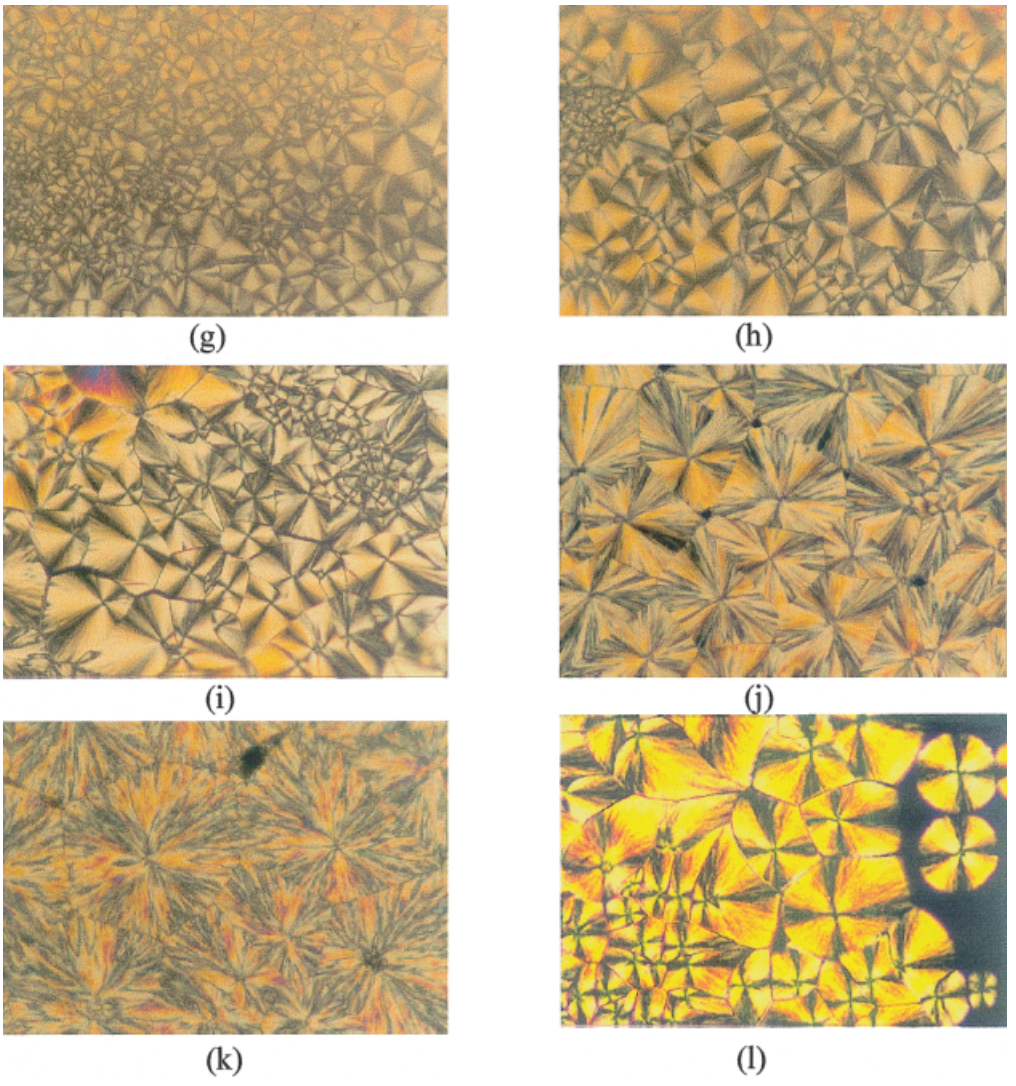

Figure 1 (*Continued from the previous page*)

oven at 100°C for 12 h. Dried pellets were heated on a hot press between a cover glass and a Teflon film at 270°C for 10 min, and then compressed at 2500 psi for 2min. The resulting specimen was then quickly quenched into a silicone oil bath at a specific temperature ranging from 20 to 200°C. PBT melt was also quenched in ice water to prepare the nearly amorphous specimens. The thickness of the resulting films was typically below 100 μm. Solution-cast films were prepared from a 10% solution of tetrafluoro acetic acid (TFA) in CCl_4.

For microscopic observation and wide-angle X-ray diffraction (WAXD), thin films were molded with less than 100 μm of thickness. The glass fiber-filled PBT composite systems were investigated in this study containing 0, 10, 20, and 30 wt % of glass fiber, each referred as PBT0, PBT10, PBT20, and PBT30, respectively.

Wide-angle X-ray scattering (WAXS) was performed with a general area diffraction detector system (GADDS) (Bruker) equipped with a collimator having the diameter of 0.2 to 0.5 mm. CuKα (λ = 1.541 Å) radiation was utilized for all X-ray experiments scanning from 5 to 45° (2θ). The crystalline structures of the prepared samples were examined by using a transmission polarized optical microscope (Nikon).

Dynamic mechanical thermal analysis (DMTA) was performed by using Rheometric Scientific Mark IV in a tension mode over the temperature range from −50 to 250°C. The storage modulus, G', and loss modulus, G'', were recorded automatically by the system for data acquisition and analysis. The heating rate was 5°C/min, and frequency was fixed at 1 and 5 Hz.

RESULTS AND DISCUSSION

PBT morphology from different crystallization conditions

Figure 1 shows the spherulite morphology of PBT thin films crystallized at various crystallization temperatures (T_c) and preparation methods. The well-defined

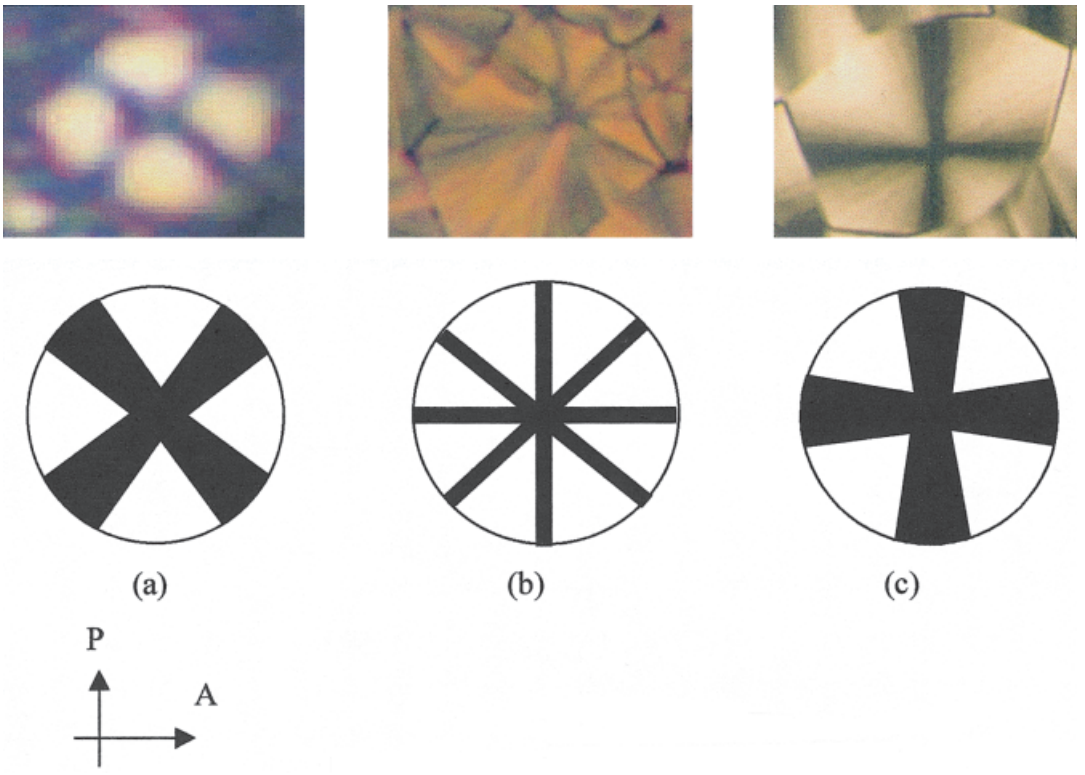

Figure 2 Maltese cross patterns of PBT spherulites crystallized at different conditions exhibiting different polarization types: (a) 45° maltese cross (unusual type) from low-temperature melt, (b) milex type from high-temperature melt, and (c) 90° maltese cross (usual type) from solution. [Color figure can be viewed in the online issue, which is available at www.interscience.wiley.com.]

spherulites can be seen when T_c is between 0 to 100°C, but nonspherical crystals can be observed with smooth boundaries of impingement when T_c is between 120 and 200°C. It has been reported that the spherulite boundaries examined by transmission electron microscopy have irregular features.[27] Low molar mass species have been found to accumulate in the spherulite boundaries resulting in brittle layers in mechanical fracture due to the increased amount of low molar mass species. In this study, however, the boundaries of matured spherulites appear to maintain spherical shape before and after the spherulite impingement and no low-molecular-mass species or impurities are not clearly observed at the boundary layers.

Comparing the spherulitic morphologies obtained from the melt [Fig. 1(a)–(k)] and from solution [Fig. 1(l)], the morphological difference is quite noticeable. As shown in Figure 1(a)–(i), all the melt-crystallized PBT films show the maltese crosses with 45° to the polarizers, which is known as an unusual type of sperulite. This unusual type is a characteristic of spherulites whose optical axis lies at an angle of approximately 45° to the spherulitic radius.[28,29] On the other hand, as seen in the solvent-crystallized PBT films in Figure 1(l), the maltese crosses are along the polar direction (0° and 90°) under the polarized microscope, referred to as na usual type. It arises from spherulites containing their optical axis either along or perpendicular to the spherulitic radius. When T_c =180 and 200°C, however, the cross patterns exhibit a mixture of the unusual and usual types of spherulites.

As a summary, the characteristic features of PBT spherulites are shown in the Figure 2, representing different maltese cross patterns referred to different crystallization conditions. The 45° maltese cross (unusual-type) spherulites in Figure 2(a) are formed at low temperatures, and the 90° maltese cross (usual-type) spherulites are likely to develop from the solution [Fig. 2(c)]. When the temperature is higher than 180°C, both types of spherulites seem to be formed as in Figure 2(b).

The spherulite size measured from the optical micrograph is shown in the Figure 3 ploted as a function of T_c. As T_c increases, the crystal size increases in an accelerating fashion indicating that the crystal may grow as large as it could in a hypothetical thermal condition, for example, over 200°C. It should be noticed that the degree of crystallinity usually exhibits a asymptotic value with crystallization temperature. Therefore, the crystal may grow big in size while the number of crystal is low in a way of maintaining the asymptotic degree of crystallinity with respect to crys-

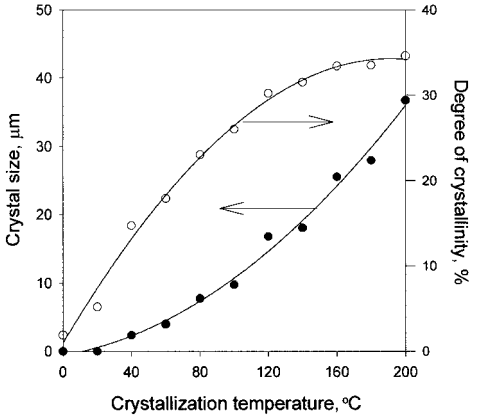

Figure 3 Crystal size and degree of crystallinity of PBT spherulites as a function of crystallization temperature.

tallization temperature. The degree of crystallinity shown in this figure will be discussed later.

Morphology of glass fiber-reinforced PBT composites

The foreign bodies, such as nucleating agents, fibers, or particulate fillers, usually provide extra active sites, which usually enhance the initiation of crystallization, although some nucleation may originate from local tangling of ordering of polymer chains. The number of nucleation sites often determines the morphology of growing crystallites because a large number of nucleation centers would lead to a large number of small crystallites. Figure 4 shows the crosspolar optical micrographs of melt-crystallized PBT composites. Figure 4(a) and (b) depicts the ice-water quenched films, while Figure 4(c) and (d) the air-cooled films. It can be clearly seen that glass fibers provide nucleating sites when they are used as a reinforcementof PBT composites. PBT0 contains relatively large and distinguishable crystals, whereas a dense granular texture of crystals is formed in the vicinity of glass fibers. The number density along the fiber surface is much greater than that in the bulk, but the size of spherulites on the fiber surface is smaller.

Because the spherulites can be seen in ice water-quenched samples, it may be concluded that a perfectly amorphous state of PBT specimen may not be achieved in a practical range of cooling rates. In addition, the spherulite size of films quenched in ice water [Fig. 4(a) and (b)] is much smaller than that quenched

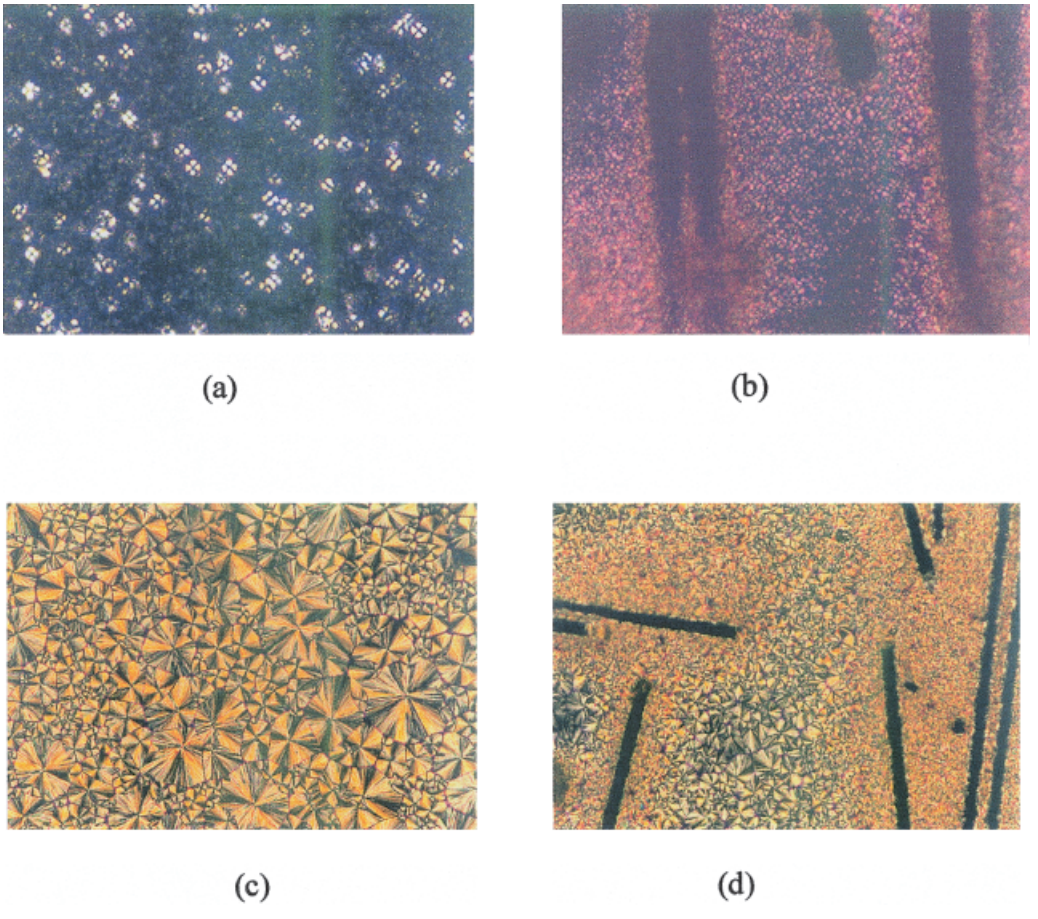

Figure 4 Optical micrograph comparison of melt-crystallized films of PBT polymer (PBT0) in (a) and (c), and glass fiber-reinforced PBT composite (PBT30) in (b) and (d). Crystallization cooling conditions by ice water quenching in (a) and (b), and natural-air cooling in (c) and (d). [Color figure can be viewed in the online issue, which is available at www.interscience.wiley.com.]

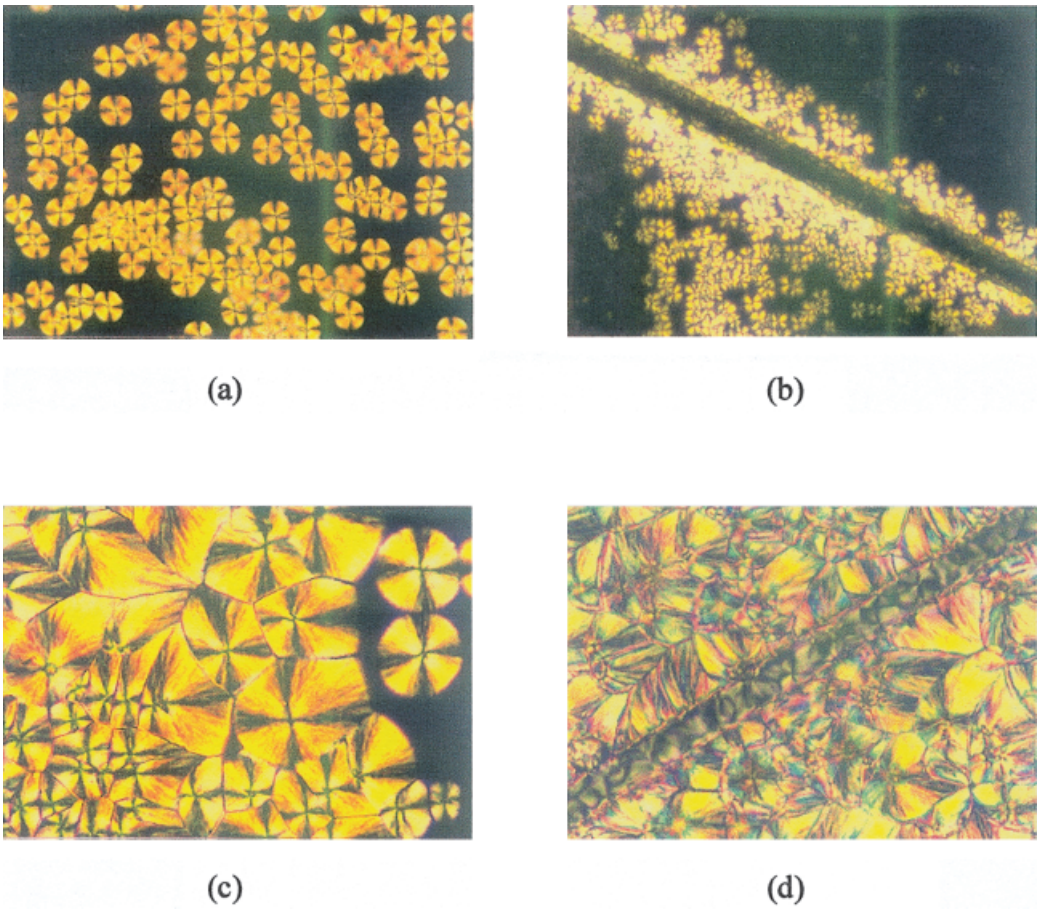

Figure 5 Optical micrograph comparison of solvent-crystalized films of PBT polymer (PBT0) in (a) and (c), and glass fiber-reinforced PBT composite (PBT30) in (b) and (d). Crystallization cooling conditions by ice water quenching in (a) and (b), and natural-air cooling in (c) and (d). [Color figure can be viewed in the online issue, which is available at www.interscience.wiley.com.]

in air [Fig. 4(c)and (d)]. It demonstrates that the crystallization rate of PBT systems is so fast that the crystallization of PBT is nearly unavoidable, and it should be mentioned that the resulting morphology is strongly affected by the cooling rate and temperatureee in polymer manufacturing processes.

Figure 5 shows the solvent-crystallized films comparing the pristine PBT polymer [Fig. 5(a) and (c)] and its composite [Fig. 5(b) and (d)}. Figure 5(a) and (b) shows ice water-quenched samples, and Figure 5(c) and (d) air-cooled samples. It can be seen that the size of spherulites around the glass fiber is smaller than that in the bulk, and the number density of crystal is higher at the fiber surface than in the bulk. However, it should be mentioned that the transcrystalline is not clearly observed around the fiber surfaces in both cases of solvent- and melt-crystallized PBT films. This indicates that the nucleation density is increased by the fiber surface, but it may not be sufficient enough to form transcrystalline layers. This result is agreed with other investigations.[16–18]

Crystallinity determination by WAXD analysis

The Ruland method has often been used as a fundamental method to evaluate the polymer crystallinity.[30] The correction factor (K) included in Ruland equation has been estimated by integrating the scattering factor and disorder function in the selected s-range (s_0–s_1), viz:

$$K = \frac{\int_{s_0}^{s_1} s^2 f^2 \, ds}{\int_{s_0}^{s_1} s^2 f^2 D^2 \, ds} \tag{1}$$

where $s = (2\sin\theta)/\lambda$, λ is wavelength, D is disorder function, and $\bar{f}^2$ is the mean-square atomic scattering factor for the polymer. As proposed for the first-order defects (e.g., thermal vibrations), the disorder function was assumed as:[30]

$$D^2 = \exp(-ks^2) \tag{2}$$

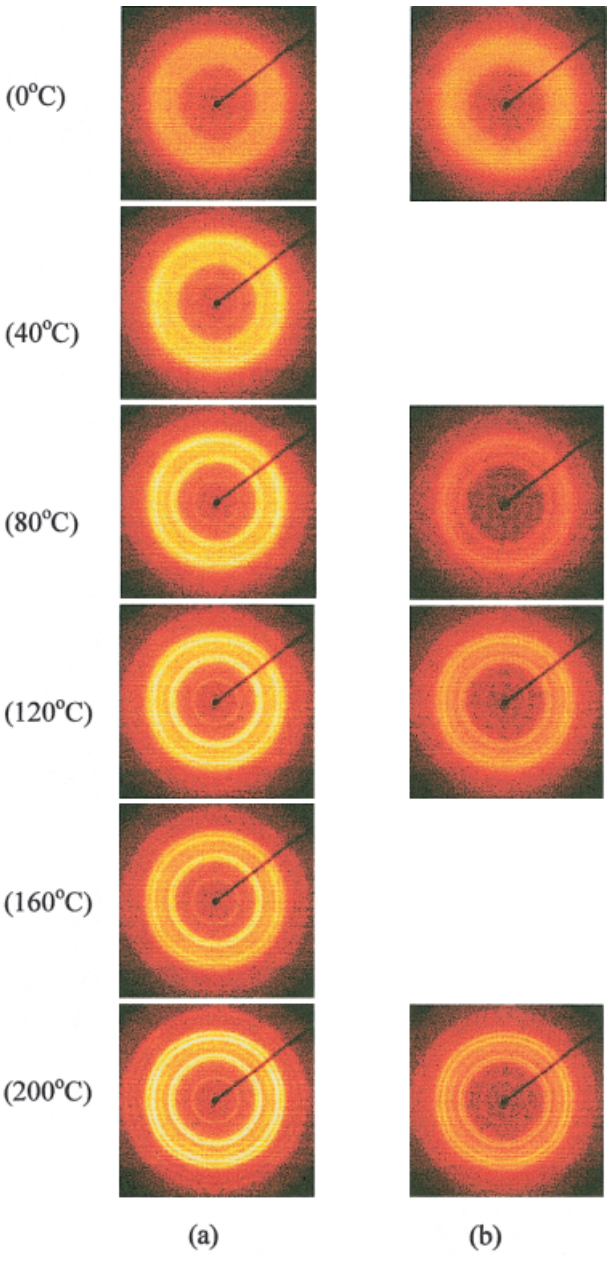

Figure 6 WAXD pattern of (a) PBT polymer (PBT0) and (b) glass fiber-reinforced PBT composite (PBT30) cyrstallized at indicated T_c. [Color figure can be viewed in the online issue, which is available at www.interscience.wiley.com.]

where k is a constant. It should be mentioned that K values may be evaluated for different values of k specified in different range of s or different forms of disorder functions.

Figure 6 shows the X-ray diffraction pattern of PBT0 and PBT30 composite systems crystallized at various T_c. The pattern of the film crystallized at 0°C shows a diffuse halo without a clear evidence of crystalline orientation. As T_c is increased, the pattern exhibits intense crystalline reflections indicating both increased crystallinity and increased crystalline size. The same trend can be seen in the diffraction patterns for composites (PBT30), but they are relatively diffused to the polymer (PBT0), seemingly due to scattering by glass fibers.

Figure 7 shows typical WAXD patterns for the films crystallized isothermally from the polymer melt. Strong diffraction peaks and several weak peaks are observed for the samples crystallized above 40°C, but, there are no distinct peaks observed $T_c < 20$°C, indicating the film in the nearly amorphous phase. The observed and calculated d-spacings are summarized in Table I. No reflections of characteristics of the *all-trans* form are identified.[31] It should be mentioned that there can be seen a peak at $2\theta = 39.538°$ only when the crystallization temperature is above 180°C, and it becomes stronger as the crystallization temperature is increased. As discussed in Figure 2, the 90° maltese cross pattern begins appearing at $T_c > 180$°C, and it is mixed with the 45° cross pattern. Further research should be performed to validate the relationship between the type of PBT crystal structure and the crystallographic observation.

Using the Ruland's method for estimating the crystallinity of the isothermally crystallized films, I(2θ) curves are transformed into $s^2I(s)$ curves and resolved into the background. The analysis results are summarized in Table II for $k = 0$ and $k = 7$.[32] Table II shows that the degree of crystallinity of PBT0 is about 0.02 to 0.346 in the range of 0°C $< T_c <$ 200°C with a disorder parameter $k = 7$. As a result of this analysis, the degree of crystallinity can be seen as a function of T_c in Figure 3. As the crystallization temperature increase, the degree of crystallinty approaches 35%, which agrees well with the degree of crystallinity of 36% at 200°C estimated by the density measurement.[8]

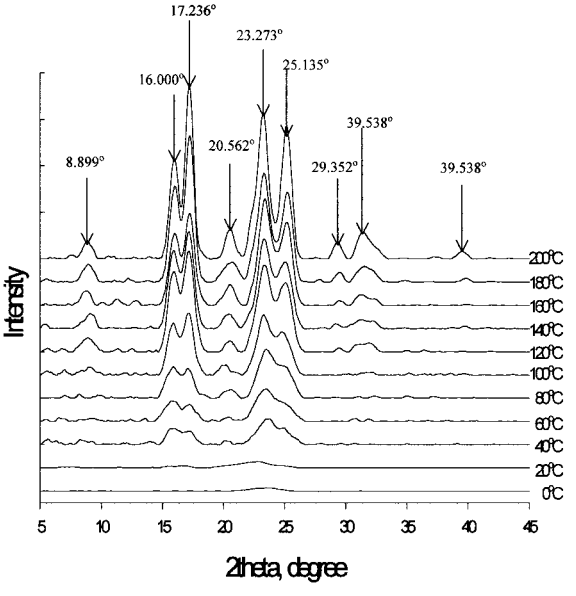

Figure 7 Comparison of WAXD peak patterns of PBT polymer (PBT0) crystallized at indicated T_c.

TABLE I
Experimental and Theoretical d-Spacings for PBT Triclinic Unit Cell [a = 4.83 Å (99.9°); b = 5.95 Å (64.6°); c = 11.67 Å (69.4°)]

	Measured		Calculated		
I/I_0	Angle 2-theta^0	d-Spacing angstrom	Angle 2-theta^0	d-spacing angstrom	*hkl*
mw	8.899	9.929	9.116	9.7	$00\bar{1}$
ms	15.981	5.541	16.100	5.50	$10\bar{1}$
s	17.236	5.140	17.220	5.15	$01\bar{0}$
m	20.562	4.316	20.506	4.33	$10\bar{2}$
vs	23.274	3.819	23.190	3.83	$10\bar{0}$
vs	25.135	3.540	25.371	3.51	$02\bar{1}$
vw	29.352	3.040	27.442	3.25	$00\bar{3}$
w	31.457	2.842	30.720	2.91	$11\bar{3}$
vw	39.538	2.277	39.344	2.29	$10\bar{5}$

Viscoelastic characterization

Figures 8, 9, and 10 show the complex moduli of PBT samples crystallized at different temperatures. As can be seen, the glass transition temperature decreases with the degree of crystallinity, for example, T_g = 64°C at X_c = 2.0% and T_g = 89°C at X_c = 34.6% as measured by tan δ in Figure 10. As discussed in the literature, T_g of crystalline polymers may increase or decrease with crystallinity depending on the nature and the role of cyrstalline phase in the glass transition process.[33,34] For the PBT system used in this study, it is clearly seen that the glass transition temperature decreases with crystallinity.

In addition, the elastic modulus increases due to the increased degree of crystallization in the all the temperature ranges of DMTA measurement.[35] In particular, the increment of the modulus in the rubbery state of PBT over T_g seems more than one order of magnitude approximately from 10^8 to 10^9 dyne/cm^2, depending on the degree of crystallinity. The elastic modulus drops at the main crystalline melting temperature around 230°C, which is often referred as the α transition. The characteristic temperatures measured by the dynamic mechcanical tests and the crystallinity obtained by WAXS are summarized in Table III.

Crystalline polymers have a damping peak corresponding to the glass transition as well as crystalline melting. As can be seen in Figure 9 and 10, the intensity of tan δ at the glass transition is reduced with T_c, indicating that the more the crystalline phase exists in the sample, the lower the intensity and damping of glass transition. It can also be interpreted that the time lag between the applied stress and strain is reduced as the crystallinity is increased, resulting in more elastic feature of the sample.

In addition to the damping peak of T_g, tan δ and G'' show another peak located between the glass transition and the melting temperature in the region of T_c is between 80 and 160°C. It may be ascribed to the melting of a different or additional crystalline phase induced by annealing.[6,35] This peak seems to increase with the annealing temperature, but it appears at a temperature higher than the annealing temperature. This transition in PBT does not appear when T_c is lower than 80°C or higher than 160°C in this study. Although they are not included here, the DSC exper-

TABLE II
Crystallinity, X_c as a Function of *k* and Integration Interval

		Integration interval, $s_0 - s_P$					
T_c^0C	*k*	0.05–0.2	0.05–0.3	0.05–0.4	0.05–0.5	Mean X_c	Std. dev. ($\times 10^{-2}$)
0	0	0.022	0.021	0.014	0.008		
	7	0.023	0.025	0.018	0.012	0.020	0.578
20	0	0.051	0.049	0.033	0.027		
	7	0.058	0.053	0.052	0.051	0.052	0.121
40	0	0.136	0.131	0.108	0.096		
	4	0.147	0.155	0.143	0.144	0.147	0.536
60	0	0.174	0.160	0.127	0.114		
	4	0.188	0.189	0.168	0.171	0.179	1.110
80	0	0.216	0.198	0.167	0.155		
	4	0.233	0.234	0.220	0.233	0.230	0.637
100	0	0.245	0.223	0.198	0.168		
	4	0.265	0.263	0.261	0.252	0.260	0.567
120	0	0.282	0.261	0.226	0.197		
	4	0.305	0.308	0.298	0.296	0.302	0.570
140	0	0.293	0.278	0.230	0.209		
	4	0.316	0.328	0.304	0.314	0.315	0.503
160	0	0.312	0.286	0.253	0.219		
	4	0.337	0.337	0.334	0.329	0.334	0.412
180	0	0.311	0.290	0.256	0.217		
	4	0.347	0.342	0.338	0.326	0.335	0.709
200	0	0.321	0.397	0.262	0.226		
	4	0.347	0.350	0.346	0.340	0.346	0.477

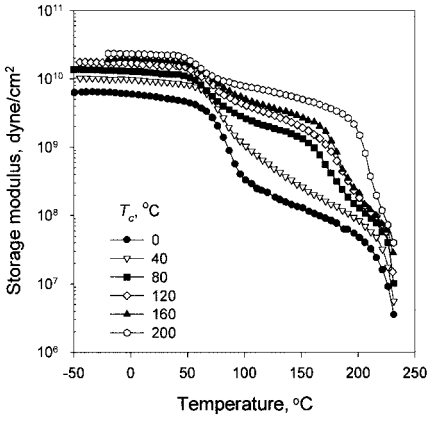

Figure 8 Storage modulus of PBT crystallized at various T_c plotted as a function of temperature.

iments also support the additional crystallization melting corresponding to the annealing process.

The effects of crystallinity on the modulus are illustrated in Figure 11. The modulus values below and above T_g were taken from the curves in Figure 8 at 0 and 100°C, respectively, where the moduli were reasonably considered to maintain the initial crystallinity irrespective of the increasing temperature in dynamic mechanical experiments. As a result of Figure 11, the modulus in the amorphous phase may be obtained by extrapolating the curves at $X_c = 0$, providing two moduli before and after the glass transition temperature: $G'_a = 3.0 \times 10^8$ Pa below T_g and $G'_a = 2.0 \times 10^7$ Pa above T_g. It demonstrates that the modulus in the amorphous phase decreases by an order of magnitude due to the increased chain mobility through the glass transition. In addition, extrapolating the two curves in Figure 11 up to $X_c = 1.0$, the value of G'_c may be obtained as 2.0×10^{10} Pa in both cases. Then, the storage modulus may be described as a function of crystallinity by the dual-phase continuity model with the one-fifth power for both crystalline and amorphous phases:[36]

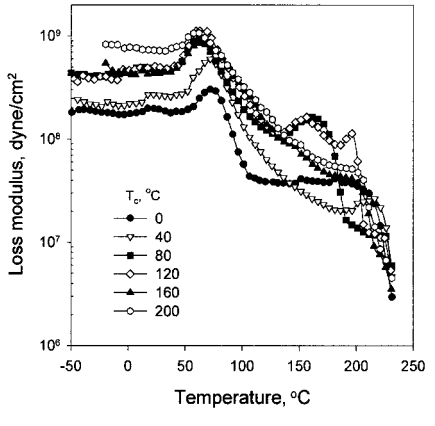

Figure 9 Loss modulus of PBT crystallized at various T_c plotted as a function of temperature.

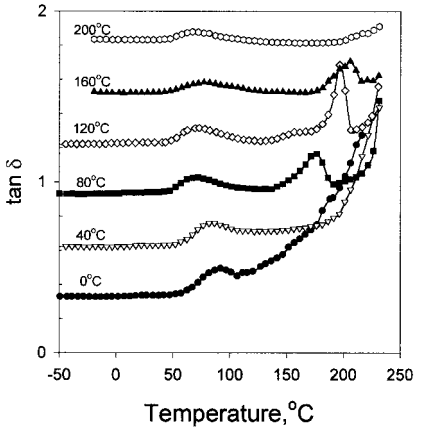

Figure 10 Dynamic damping peaks (tan δ) of PBT crystallized at various T_c plotted as a function of temperature. Curves were vertically shifted maintaining the same scale for comparison.

$$G'^{1/5} = w_a G'^{1/5}_a + w_c G'^{1/5}_c \tag{3}$$

where w_a and w_c are the weight fraction of amorphous and crystalline phases, respectively, and G'_a and G'_c being the storage moduli of the amorphous and crystalline phases, respectively. The model eq. (3) is compared well with the experimental result in Figure 11 for below and above glass transition temperature. It is interesting to note that the same value of the storage modulus of crystalline phase, G'_c, is used for the model prediction in the two cases.

To investigate the effect of crystallinity on the viscoelastic properties, the storage modulus curve obtained from the specimen crystallized at 0°C may be used as a reference state containing a minimal quantity of crystallinity that can be achieved in a practical experiment. Subsequently taking the curve at $T_c = 0$°C in Figure 8 as G'_a and the other curves in the same figure as G', eq. (3) may used to extract out G'_c to represent the modulus of the crystalline phase changing during the DMTA experiments at a constant heating rate. Rewriting eq. (3) for the storage modulus of crystalline phase as a function of temperature,

$$G'_c = \frac{1}{w_c}[(G')^{1/5} - w_a(G'_a)^{1/5}] \tag{4}$$

TABLE III
Transition Temperatures with Various Crystallization Temperature, T_c and Degree of Crystallinity, X_c

T_c °C	X_c %	$T_{g\ onset}$ °C	$T_{g\ end}$ °C	$T_{a\ onset}$ °C	$T_{a\ end}$ °C
0	2.0	57.2	111.3	—	—
40	14.7	57.1	96.4	—	—
80	23.0	49.3	91.6	151.7	206.2
120	30.2	48.4	87.9	156.7	211.3
160	33.4	47.4	86.8	166.3	220.8
200	34.6	42.3	81.7	196.3	226.3

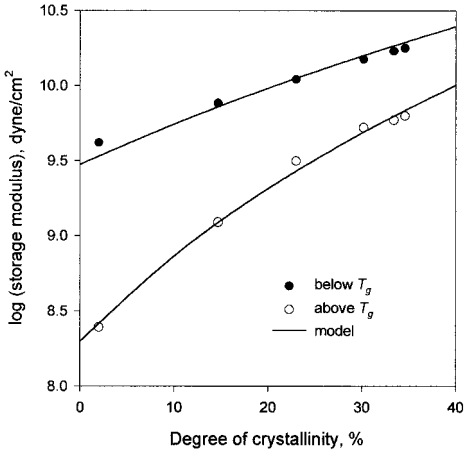

Figure 11 Storage modulus below and above T_g plotted as a function of crystallinity: data taken from Figure 8 at 0 and 100°C, respectively.

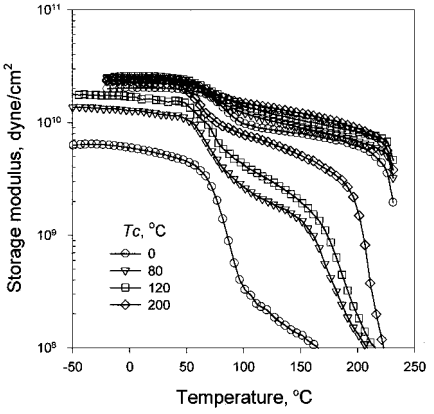

Figure 13 Comparison of PBT polymer (PBT0: lower four curves) and glass fiber-reinforced PBT composite (PBT30: upper four curves) crystallized at different T_c.

The weight fraction of each curve in Figure 12 is listed in Table III. As can be seen in Figure 12, the modulus of the crystalline phase (G'_c) maintains a constant value in the glassy state for all the curves. They decrease during the glass transition but recover their previous value right after the transition, maintaining nearly constant values until the crystalline melting starts. The modulus curve at T_c = 200°C has the highest value of crystallinity, and thus shows the highest G'_c throughout the whole range of temperature, and it decreases at the α transition of major melting of PBT. The G'_c curves obtained at 80°C $\leq T_c \leq$ 160°C exhibit lower values of modulus in the glassy and rubbery states because their degree of crystallinity is lower than the curve at T_c = 200°C. When T_c = 40°C, the crystalline phase does not show a modulus plateau in the rubbery state seemingly because the degree of crystallinity, X_c = 0.147, is not high enough to act as an effective reinforcement of PBT systems.

The effects of glass fibers on the storage modulus (upper four curves) are shown in Figure 13, where they are also compared with PBT0 (lower four curves). It can be clearly seen that the glass fibers act as a reinforcement, providing higher values of modulus throughout the whole range of temperatures. In particular, the modulus in the rubbery state maintains much higher values than pristine PBT resin. It can also be seen that the glass fiber-reinforced composites do not seemed to be much affected by the degree of crystallization or additional crystallization. Although the modulus values are altered by the degree of crystallization, they do not exhibit low-temperature melting in the temperature range between 150 and 200°C. It should also be mentioned that the α transition of the glass fiber-reinforced composites is increased by 30–50°C compared to the neat PBT resin.[35]

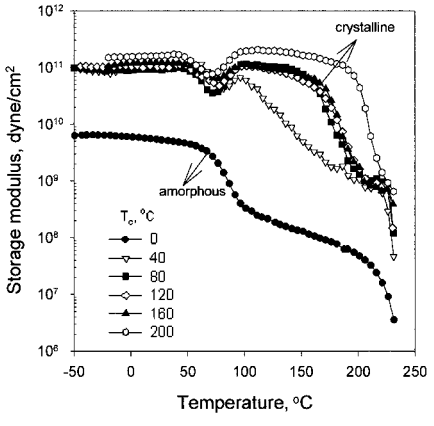

Figure 12 Calculated storage modulus of a crystalline phase using a dual-phase continuity model based on the reference state of amorphous PBT at T_c = 0°C.,

CONCLUSIONS

The crystalline morphologies of PBT thin-film composites were examined through a polarizing optical microscope (POM) in relation to the degree of crystallinity measured by the wide-angle X-ray diffraction (WAXD) experiments. A dynamic mechanical thermal analysis (DMTA) was used to identify the relationship among crystalline structures, crystallinity, and viscoelacity properties of PBT.

The morphology of PBT exhibited three different types in maltes cross pattern; 90° maltese cross (usual type) by solvent crystallization, 45° maltese cross (unusual type) by melt crystallization at lower crystallization temperature, and mixed type by melt crystallization at higher crystallization temperature above 160°C. Different types of spherulite structure showed different melting peaks and different viscoelastic characteristics. The glass fibers increased the number density and decreased the size of crystallites acting as crystallization nucleation sites. However, transcrystalline layer was not clearly observed at the vicinity of the glass fiber surfaces.

The storage modulus was analyzed by using an empirical model to extract out the effect of crystalline phase on the modulus change. The crystal-phase modulus (G'_c) was extracted out from the experimental data by using the model equation. Finally, the effect of glass fiber on the modulus of PBT composite systems was experimentally measured and compared with neat PBT resin systems in various thermal treatment conditions.

This work was supported by the Korea Science and Engineering Foundation (96-0502-0601-3).

REFERENCES

1. Burton, R. H.; Folkes, M. J. In Mechanical Properties of Reinforced Thermoplastics; Clegg, D. W.; Collyer, A. A., Eds.; Elsevier: London, 1986.
2. Park, C.-S.; Lee, K.-J.; Nam, J.-D.; Kim, S.-W. J Appl Polym Sci 2000, 78, 576.
3. Biye, C. A.; Overton, J. R. Bull Am Phys Ser 2 1974, 19, 352.
4. Jakewas, R.; Ward, I. M.; Wilding, M. A.; Hall, I. H.; Desborough, I. J.; Pass, M. G. J Polym Sci Polym Phys Ed 1975, 13, 799.
5. Mencik, Z. J Polym Sci Polym Phys Ed 1975, 13, 2173.
6. Nam, J.-D.; Seferis, J. C. J Polym Sci Polym Phys Ed 1991, 29, 601.
7. Tashiro, K.; Nakai, Y.; Kobayashi, M.; Tadokoro, H. Macromolecules 1980, 13, 137.
8. Apostolov, A. A.; Fakirov, S.; Stamm, M.; Patil, R.D.; Mark, J. E. Macromolecules 2000, 33, 6856.
9. Chou, T. W. Material Science and Technology; VCH: Weinheim, 1993; vol. 13.
10. Wunderlich, G. Macromolecular Physics; Academic Press: New York, 1976, vol.2, Chap. 5.
11. Velisaris, N.; Seferis, J. C. Polym Eng Sci 1986, 26, 1574.
12. Tung, M.; Dynes, P. J. J Appl Polym Sci 1987, 33, 505.
13. Lee, Y.; Porter, R. S. Polym Eng Sci 1986, 26, 633.
14. Cambell, D.; Qayyum, M. M. J Polym Sci Polym Phys Ed 1984, 18, 83.
15. Desio, G. P. ; Rebenfeld, L. J Appl Polym Sci 1992, 44, 1989.
16. Avela, M.; Martuscelli, E.; Sellitt, C.; Garagnani, E. J Mater Sci 1987, 22, 3185.
17. Devaux, J.; Chabert, B. Polym Commun 1990, 31, 391.
18. Janevski, A.; Bogoeva-Gaceva, G. J Appl Polym Sci 1998, 69, 381.
19. Thomason, J. L. ; Von Rooyen, A. A. J Mater Sci 1992, 27, 889.
20. Campbel, D.; Qayyum, M. M. J Polym Sci Polym Phys Ed 1980, 18, 83.
21. Varga, J.; Karger-Kocsis, J. Polym Bull 1993, 30, 105.
22. Devaux, E.; Chabert, B. Polym Commun 1991, 32, 464.
23. Vendramini, J.; Bas, C.; Merle, G.; Boissonnat, P.; Alberola, N. D. Polym Comp 2000, 21, 724.
24. Hobbs, S. Y. U.S. Pat. 3,812,077.
25. Woodward, E. Understanding Polymer Morphology; Hanser: Cincinnati, 1995.
26. Baird, D.G.; Collias, D. I. Polymer Processing; Butterworth-Heinemann,:Boston, 1995.
27. Gedde, U. W. Polymer Physics; Chapman & Hall: London, 1995.
28. Stein, R. S.; Misra, A. J Polym Sci Polym Phys Ed 1980, 18, 327.
29. Stein, R. S. In Structure and Properties of Polymer Films; Lenz, R. W.; Stein, R. S., Eds.; Plenum: New York, 1973.
30. Ruland, W. Acta Crystallogr 1961, 14, 1180.
31. Yokouchi, M.; Sakakibara, Y.; Chatani, Y.; Tadokoro, H.; Tanaka, T.; Yoda, K. Marcromolecules 1976, 9, 266.
32. Balta-Calleja, J.; Vonk, C.G. X-ray Scattering of Synthetic Polymers; Elsevier: Amsterdam, 1989.
33. Rabek, J. F. Experimental Methods in Polymer Chemistry; John Wiley & Sons: New York, 1980.
34. Brydson, J. A. Polymer Science; North-Holland: Amsterdam, 1973, vol. 1.
35. Nielsen, L. E.; Landel, R. F. Mechanical Properties of Polymers and Composites, Marcel Dekker: New York, 1994.
36. Davies, W. E. A. J Phys D 1071, 4, 318.